Unified Scheduling for Predictable Communication Reliability in Cellular Networks with D2D Links

Yuwei Xie, Hongwei Zhang, Pengfei Ren

Abstract—**Cellular networks with device-to-device (D2D) links are increasingly being explored for mission-critical industrial applications which require predictable communication reliability. With interference being a major source of packet loss, it is thus critical to control interference among concurrent transmissions in a predictable manner to ensure the required communication reliability. To this end, we propose a Unified Cellular Scheduling (UCS) framework that, based on the Physical-Ratio-K (PRK) interference model, schedules uplink, downlink, and D2D transmissions in a unified manner to ensure predictable communication reliability while maximizing channel spatial reuse. UCS also provides a simple, effective approach to mode selection that maximizes the communication capacity for each involved communication pair. UCS effectively uses multiple channels for high throughput as well as resilience to channel fading and external interference. Leveraging the availability of base stations (BSes) as well as high-speed, out-of-band connectivity between BSes, UCS effectively orchestrates the functionalities of BSes and user equipment (UE) for light-weight control signaling and ease of incremental deployment and integration with existing cellular standards. We have implemented UCS using the open-source, standards-compliant cellular networking platform OpenAirInterface, and we have validated the UCS design and implementation using the USRP B210 software-defined radios in the ORBIT wireless testbed. We have also evaluated UCS through high-fidelity, at-scale simulation studies; we observe that UCS ensures predictable communication reliability while achieving a higher channel spatial reuse rate than existing mechanisms, and that the distributed UCS framework enables a channel spatial reuse rate statistically equal to that in the state-of-the-art centralized scheduling algorithm iOrder.**

I. INTRODUCTION

Long-Term Evolution Advanced Pro (LTE-Advanced Pro) and 5G cellular networks with device-to-device (D2D) communications are increasingly being explored for mission-critical industrial applications such as real-time control and Augmented-Reality/Virtual-Reality (AR/VR) [1], [2], [3]. For instance, close-by sensors, controllers, and actuators in a factory cell may communicate with one another in a D2D manner, whereas a technician wearing an AR head-mount-display may communicate with remote experts through the base station and Internet backbone. For these applications, predictable communication reliability is not only important by itself, it is also the basis of real-time communication since unpredictable communication reliability will make it difficult

to ensure timely delivery of messages [4], [5]. Controlling communication reliability in a predictable manner is also a basis for controlling the inherent trade-off between communication reliability, delay, and throughput, which is important for system-level optimization [4], [6]. Cellular communication, however, is subject to complex dynamics and uncertainties, and interference among concurrent transmissions is a major source of uncertainty [4], [5]. For predictable communication reliability in mission-critical cellular networks, it is critical to schedule concurrent transmissions so that interference among them is controlled in a predictable manner.

Related work. For controlling interference in cellular networks with D2D links, power control, channel assignment, and scheduling have been considered in existing studies [7], [8], [9], [10], [11], [12], [13], [14], [15], [16], [17], [18], [19], [20], [21], [22]. The existing cellular technology LTE has also defined the High Interference Indicator (HII) and Overload Indicator (OI) for uplinks as well as Relative Narrowband Transmit Power (RNTP) for downlinks in order for a cell to inform neighboring cells of the Resource Blocks (RBs) that are susceptible to interference [23]. For more precise interference control in coordinated multi-point (CoMP) transmission and reception, LTE has also defined coordinated scheduling mechanisms such as dynamic point blanking which dynamically prevent transmission at certain time-frequency resource. The existing mechanisms, however, do not ensure predictable interference control and communication reliability due to the following reasons: considering single-cell settings only without addressing inter-cell interference [9], [10], [11], [12], using inaccurate interference models [7], [8], [13], [14], assuming uniform wireless channel fading across networks which is unrealistic in practice [15], [16], assuming exclusion-regions around receivers without mechanisms for identifying the exclusion-regions in practice [9], not considering the interference from cellular-mode transmitters to D2D receivers [17], not considering interference between D2D links [18], not considering inter-cell interference among cellular and D2D links [19], [24], only considered downlink transmissions [20], and/or maximizing throughput without addressing reliability-throughput tradeoff (i.e., achieving maximum network throughput tends to require increasing channel spatial reuse, which in turn reduces per-transmission reliability) [9], [10], [11], [20], [21], [22], [5], [4]. Several pieces of work [19], [24] do not consider spectrum reuse across D2D links either, which unnecessarily reduces achievable network capacity.

Wireless networks such as those based on WirelessHART, ISA100.11p, WIA-PA, and IETF 6TiSCH [25], [26] have

been studied for industrial applications. Focusing on low-rate wireless networks based on IEEE 802.15.4/4e, those studies do not focus on cellular networks with D2D links, nor have they focused on distributed scheduling with predictable interference control and maximum channel spatial reuse [4].

Contributions of this work. Towards predictable communication reliability in industrial cellular networks with D2D links, we propose a Unified Cellular Scheduling (UCS) framework and we make the following contributions:

- Based on the Physical-Ratio-K (PRK) interference model which is suitable for developing field-deployable distributed scheduling algorithms [5], our UCS framework schedules uplink, downlink, and D2D transmissions in a unified manner to ensure predictable communication reliability while maximizing channel spatial reuse and allocating communication resources to uplink, downlink, and D2D transmissions on a need basis. UCS also provides a simple, effective approach to mode selection that maximizes the communication capacity for each involved communication pair.
- Extending the distributed scheduling protocol PRKS [4] to multi-channel settings, UCS effectively uses multiple communication channels for high throughput as well as for resilience to channel fading and external interference.
- To leverage the computational power of base stations (BSes) as well as high-speed, out-of-band connectivity between BSes, UCS places the scheduling decisions at BSes and having UEs share their local state information with corresponding BSes at relatively low-frequencies. This BS-UE functional orchestration mechanism enables light-weight control signaling, and it facilitates incremental deployment of UCS as well as technology evolution.
- We have implemented UCS using the open-source, standards-compliant cellular networking platform OpenAirInterface. We have validated the OpenAirInterface implementation of UCS using the USRP B210 software-defined radios and of the ORBIT wireless testbed. We have also studied the behavior of UCS using at-scale, high-fidelity simulation. We have observed that, unlike existing mechanisms which cannot enable predictable communication reliability, UCS ensures predictable communication reliability while achieving higher channel spatial reuse rate. We have also observed that the distributed UCS scheduling framework enables a channel spatial reuse rate statistically equal to that in the state-of-the-art centralized scheduling algorithm iOrder [27].

The rest of the paper is organized as follows. Section II presents the system model, problem specification, PRK interference model, and PRK-based scheduling protocol PRKS. Section III presents our Unified Cellular Scheduling (UCS) framework. Section IV presents the implementation of UCS in the OpenAirInterface. We evaluate UCS in Section VI and V, and we summarize our concluding remarks in Section VII.

II. PRELIMINARIES

A. System Model and Problem Specification

We consider cellular networks of multiple cells where each cell has a Base Station (BS) and a number of user equipment (UEs). Each cell has a set of uplinks (i.e., transmissions from UEs to the BS) and downlinks (i.e., transmissions from the BS to UEs). A UE may also transmit data to another UE in the network. The transmission from one UE to another can be in cellular mode (i.e., an uplink transmission followed by a downlink transmission) or in D2D mode where the transmitter UE sends data directly to the receiver UE without using any BS in data delivery. If a UE sends data directly to another UE, we regard the communication link as a D2D link. In line with the current wireless systems, e.g., LTE-type systems, the basic resource allocation unit is Resource Block (RB), which consists of 12 consecutive subcarriers in the frequency domain and one 0.5ms time slot in the time domain, with each subcarrier occupying a 15KHz spectrum and the central frequencies of two consecutive subcarriers separated by 15KHz. For convenience of exposition, we regard the 12 consecutive subcarriers of a RB as one carrier. According to the LTE standard, each cell may use multiple component carriers, with each component carrier consisting of 6 - 100 carriers (i.e., with bandwidth ranging from 1.4MHz to 20MHz) [23]. For reducing scheduling overhead, the LTE standard also groups a certain number of carriers into a carrier group, and the specific grouping methods depend on the bandwidth of a component carrier.

The uplinks, downlinks, and D2D links of a cellular network share the wireless spectrum available. The objectives of this work are to develop 1) an algorithm that, for each UE-to-UE communication pair, decides whether the communication shall be in cellular mode or D2D mode for maximum communication throughput while satisfying the required communication reliability, and 2) an algorithm that, given a time slot and the set of uplinks, downlinks, and D2D links (if any), schedules a maximal subset of the links to transmit at the time slot so that the required communication reliability is guaranteed.

As a first-step towards field-deployable solutions that ensure predictable communication reliability in cellular networks with D2D links, we consider mostly-immobile networks where UEs are fixed at specific locations most of the time even though they may be moved around infrequently. In such networks, the average background noise power and the average wireless path loss tend to be stable at timescales of seconds, minutes, or even longer [4]. Focusing on the problem of transmission scheduling, we assume that transmission power for each node (i.e., BS or UE) is fixed, even though different nodes may use different transmission powers. For highly mobile networks (e.g., those with vehicles) and transmission power control, techniques such as those by Li et al. [28] and Wang et al. [29] may be applied, but detailed study is beyond the scope of this work.

B. Interference Model

For predictable interference control in transmission scheduling, we adopt the Physical-Ratio-K (PRK) interference

model [23] in our study. The PRK model integrates the protocol model's locality with the physical model's high-fidelity, and it is suitable for designing distributed scheduling protocols that ensure predictable interference control in the presence of dynamics and uncertainties. As shown in Figure 1, in the PRK model, a node C' is regarded as not interfering and thus can transmit concurrently with the transmission form another node S to its receiver R if and only if $P(C', R) < \frac{P(S,R)}{K_{S,R,T_{S,R}}}$, where $P(C', R)$ and $P(S, R)$ is the average strength of signals reaching R from C' and S respectively, $K_{S,R,T_{S,R}}$ is the minimum real number chosen such that, in the presence of cumulative interference from all concurrent transmitters, the probability for R to successfully receive packets from S is no less than the minimum link reliability $T_{S,R}$ required by applications. The PRK model defines, for each link (S, R), an exclusion region $\mathbb{E}_{S,R,T_{S,R}}$ around the receiver R such that a node $C \in \mathbb{E}_{S,R,T_{S,R}}$ if and only if $P(C, R) \geq \frac{P(S,R)}{K_{S,R,T_{S,R}}}$.
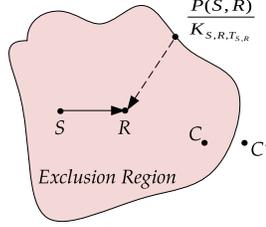

Fig. 1. PRK interference model

For predictable interference control, the parameter $K_{S,R,T_{S,R}}$ of the PRK model needs to be instantiated for every link (S, R) according to in-situ, potentially unpredictable network and environmental conditions. In particular, if the communication reliability is below (or above) $T_{S,R}$, $K_{S,R,T_{S,R}}$ needs to be increased (or decreased) so that the average interference power at the receiver R is decreased (or increased) accordingly. To this end, Zhang et al [4] have proposed a control-theoretic apporach by which each link (S, R) computes the desired change of receiver-side interference power $\Delta I_R(t)$ at a time instant t based on the in-situ measurement feedback of the actual communication reliability from S to R. If $\Delta I_R(t) < 0$ (or $\Delta I_R(t) > 0$), the link decides to increase (or decrease) $K_{S,R,T_{S,R}}$ such that the sum of the average interference power from all the nodes newly added to (or removed from) the exclusion region $\mathbb{E}_{S,R,T_{S,R}}$ is no less (or more) than $|\Delta I_R(t)|$. For every link (S, R), using its instantiated PRK model parameter $K_{S,R,T_{S,R}}$ and the local signal maps that contain the average signal power attenuation between S, R and every other close-by node C that may interfere with the transmission from S to R, link (S, R) and every close-by node C become aware of their mutual interference relations. Based on nodes/links' mutual interference relations, non-interfering transmissions can be scheduled to ensure the required communication reliability across individual links.

PRK-based scheduling has been shown to enable predictable interference control in single-channel ad hoc networks [4], [28]. In this work, we will verify the suitability and address the challenges of applying the PRK model to scheduling in multi-channel cellular networks with D2D links.

For ease of reference, Table I summarizes the key notations and abbreviations used in the paper.

Notation	Meaning
BS	Base Station
UE	User Equipment
RB	Resource Block
UCS	Unified Cellular Scheduling
PRK	Physical-Ratio-K
ICIC	Inter-cell interference coordination
$K_{S,R,T_{S,R}}$	PRK model parameter for link (S, R)
$T_{S,R}$	Minimum communication reliability required for link (S, R)
$P(A, B)$	Average strength of signals reaching B from A
$\mathbb{E}_{D2D}$	Exclusion region of a link when it operates in D2D mode
$\mathbb{E}_{up}$	Exclusion region of an uplink
$\mathbb{E}_{down}$	Exclusion region of a downlink
R_k	Reward random variable associated with a decision/arm k in model selection
μ_k	Mean value of R_k
$R_{real}(T)$	Realized regret after T plays, for a given strategy
$S_{k,t}$	Number of reward observations for arm k by time t
$D_{k,t}$	A control number for arm k at time t

TABLE I
KEY NOTATIONS AND ABBREVIATIONS

III. UNIFIED CELLULAR SCHEDULING FRAMEWORK

A. Overview

For scheduling with predictable communication reliability in cellular networks, a fundamental task is to identify the interference relations between uplinks, downlinks, and D2D links (if any). Given that the PRK interference model is a high-fidelity model specifically designed for distributed protocol design in dynamic, uncertain network settings [5] and considering the demonstrated predictable interference control in PRK-based scheduling for single-channel ad hoc networks [4], we adopt the PRK interference model in our design. The PRK model is a generic model, and it is applicable to communication links of different technologies. In particular, the impact of different communication technologies (e.g., modulation and coding schemes, multi-antenna systems) is captured by the relation between the packet-delivery-reliability (PDR) and signal-to-interference-plus-noise-ratio (SINR) for a link, and the PDR-SINR relation is used to instantiate the PRK model for each link [4]. Therefore, with the PRK model instantiated for the uplinks, downlinks, and D2D links (if any) of a cellular network, the PRK model serves as a unified approach to modeling interference relations between uplinks, downlinks, and D2D links despite the differences between these links (e.g., different types of transmitter/receiver radios). Accordingly, with inter-link interference relations identified, the cellular network scheduling problem is transformed into a unified problem of identifying maximal independent sets in a conflict graph capturing the inter-link interference relations, thus enabling maximizing spectrum spatial reuse while ensuring predictable communication reliability.

The availability of multiple communication channels (e.g., carriers) in cellular networks introduces the scalability challenge of PRK-based scheduling (e.g., in control signaling overhead), and it also provides the opportunity of channel-hopping for increased resilience against channel fading and external interference. In general, a link may maintain one PRK model parameter K for a group of n channels (e.g., carrier, carrier group, or component carrier), and the choice

of n reflects the tradeoff between control signaling overhead, data communication performance, and ease of implementation with existing LTE standard framework and thus incremental deployment. We will analyze the tradeoff in Section III-B, and we will present a PRK-based multi-channel scheduling algorithm that leverages channel hopping to balance communication load across multiple channels and to increase resilience against channel fading and external interference.

The PRK model unifies the scheduling of uplinks, downlinks, and D2D links in cellular networks, thus PRK-based cellular network scheduling bears similarity to that in ad hoc networks and provides a unified framework for reasoning about interference-control-oriented wireless network scheduling. In addition, the availability of BSes and high-speed, out-of-band interconnections between BSes (e.g., wired optical networks) in cellular networks provide unique opportunities of orchestrating the functionalities of BSes and UEs in ways to reduce control signaling overhead and to facilitate incremental deployment and technology evolution.

Figure 2 shows the architecture of the Unified Cellular Scheduling (UCS) framework. In the architecture, based on
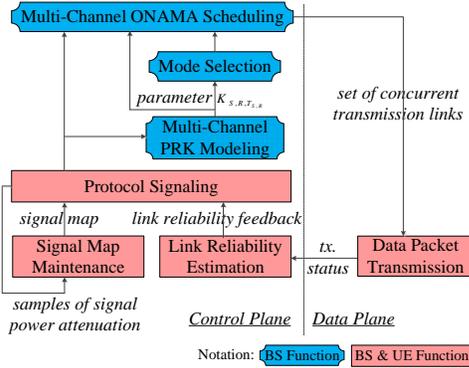

Fig. 2. UCS architecture

the status (i.e., success or failure) of uplink transmissions as well as downlink and D2D link transmissions, the BSes and UEs estimate the uplink communication reliability as well as the downlink and D2D link communication reliability respectively. Then, through collaborative control signaling, close-by nodes (i.e., BSes and UEs) estimate the average channel gain between themselves and use local signal maps to record such estimates. To facilitate incremental deployment and technology evolution, we keep the functionality of UEs to the minimum, and UEs share their communication reliability estimates and local signal maps with their respective BSes. This way, the BSes collectively have all the information needed to estimate the PRK model parameters of uplinks, downlinks, and D2D links and then make decisions on mode selection and transmission scheduling. Then, each BS can inform the corresponding UEs of the transmission modes and schedules using existing LTE signaling mechanisms or their simple extensions. In what follows, we elaborate on the design and key components of the UCS framework.

B. Multi-Channel PRK Modeling

PRK-based scheduling guarantees predictable communication reliability by maintaining one PRK model parameter K

for each channel in ad hoc networks, but it is neither practical nor necessary in cellular networks with D2D links. In the LTE-type systems, each component carriers may contain up to 100 carriers and each cell may have multiple component carriers, which means there are hundreds of channels for each link. For maintaining one K for each channel, a node needs to transmit the average channel gain between itself and neighboring nodes for each channel to the BS. In this situation, the number of pieces of control information can reach tens of thousands in each feedback period. The excessive control information will occupy resources for data transmission, resulting in scheduling delay and reducing overall system throughput. Consequently, maintaining one K for each channel is not practical in the LTE-type cellular networks.

To reduce control signaling overhead, LTE defines the carrier group as the scheduling unit depending on the bandwidth of the component carrier, which means that BSes do not need to know the channel gain for each carrier. Maintaining one K for each channel in cellular networks may not be able to further improve the accuracy of interference control, and it will also introduce control signaling overhead.

Maintaining one K for too many carriers, however, will increase the number of control steps needed for the system to converge. When a new link requests transmissions or when environment changes, inaccurate K may incorrectly add nodes to an exclusion region or delete nodes from it due to the differences of those carriers in the frequency domain, which means the scheduler needs more steps to make the value of K converge. The average link communication reliability will be affected by the increased convergence time. Consequently, the number of carriers sharing a common PRK model parameter K should be properly selected to guarantee control accuracy.

UCS maintains one K for a certain number of adjacent carriers on one component carrier to guarantee predictable communication reliability. As we will show in Section III-E, the availability of multiple carriers for a shared K enables UCS to use channel hopping to increase resilience against channel fading and external interference for improved communication reliability. Experiments have shown that a suitable number of carriers sharing one K can not only guarantee predictable communication reliability but reduce control signaling overhead greatly. For example, consider the scenario where 20 UEs share a component carrier with 100 carriers. If it maintains one K for each carrier, each UE needs to transmit $19 \times 100 = 1,900$ pieces of information about average channel gains, and the whole system needs to transmit $1,900 \times 20 = 38,000$ pieces of average channel gain information during each feedback period. If it maintains one K for every 25 adjacent carriers while also guaranteeing predictable communication reliability, each UE just needs to transmit $19 \times 4 = 76$ average channel gain information and the whole system needs to transmit $76 \times 20 = 1,520$ pieces of average channel gain information during each feedback period. The control information will be reduced by more than 90%.

For each link (S, R), the PRK model parameter K is initialized such that the initial exclusion region around the receiver R includes every strong interferer whose concurrent transmission alone in the same carrier as that of (S, R)

can make the communication reliability along (S, R) drop below the required reliability $T_{S,R}$. After its initialization, the PRK model parameter is adapted according to in-situ network and environmental conditions to ensure the required communication reliability, and the adaptation uses the regulation feedback control mechanism of Zhang et al. [4] which we have discussed in Section II-B. The method of Zhang et al. [4] was proposed for single-carrier networks. In cellular networks of N wireless carriers and using the scheduling algorithm to be presented in Section III-E shortly, a link uses a specific carrier at a time slot in probability $\frac{1}{N}$. Assuming that the average strength of the interference signal from an interferer C to the receiver R is $P(C, R)$ when both C and R are in the same communication carrier, the expected interference from C to R shall be computed as $\frac{P(C,R)}{N}$ (instead of as $P(C, R)$ in the original feedback control mechanism [4]) since C may not use the same carrier as R.

C. Mode Selection

The task of mode selection for a UE-to-UE communication pair is to decide whether the two UEs shall communicate with each other directly (i.e., in the D2D mode) or through the base station (i.e., in the cellular mode). The decision shall be made to accommodate as many concurrently-transmitting links as possible for a given communication reliability requirement. Consequently, a UE needs to choose a transmission mode that allows more links to transmit concurrently with it. To this end, the mode selection question becomes a comparison of the number of concurrent links between the D2D mode and cellular mode. The PRK model provides a good basis for addressing this issue because the value of K exactly determines which links can or cannot transmit concurrently.

From the PRK interference model, each link maintains a K to satisfy its reliability requirement, and thus each K defines an exclusion region $\mathbb{E}$. For each link (S, R), node C is in the exclusion region of the receiver R and thus shall not transmit concurrently with the transmission from S to R if and only if $P(C, R) \geq \frac{P(S,R)}{K_{S,R,T_{S,R}}}$ holds. For the D2D transmission mode, only one transmission link is needed, from the transmitter to the receiver directly. For the cellular transmission mode, two transmission links are required - an uplink followed by a downlink. This means that a UE needs to compare the number of interference links of the D2D link with the total number of interference links of both the uplink and downlink to make the decision. Consequently, the mode selection algorithm is based on the number of nodes in the exclusion region defined by K. When a pair of UEs request transmissions, the BS calculates the exclusion region for the D2D link ($\mathbb{E}_{D2D}$), uplink ($\mathbb{E}_{Up}$) and downlink ($\mathbb{E}_{Down}$) respectively according to their PRK model parameters. If $|\mathbb{E}_{D2D}| > |\mathbb{E}_{Up}| + |\mathbb{E}_{Down}|$, the UEs shall communicate through the BS in the cellular mode. If $|\mathbb{E}_{D2D}| < |\mathbb{E}_{Up}| + |\mathbb{E}_{Down}|$, the UEs shall communicate directly in the D2D mode.

To realize the above design in practice, we shall consider the fact that the values of $|\mathbb{E}_{D2D}|$ and $|\mathbb{E}_{Up}| + |\mathbb{E}_{Down}|$ for a UE-to-UE communication pair have to be learned by the UEs, the UEs cannot learn about $|\mathbb{E}_{D2D}|$(or $|\mathbb{E}_{Up}|+|\mathbb{E}_{Down}|$) unless

they communicate in the D2D (or cellular) mode, and $|\mathbb{E}_{D2D}|$ as well as $|\mathbb{E}_{Up}| + |\mathbb{E}_{Down}|$ are potentially time-varying. In particular, the mode selection problem considering these real-world challenges can be modeled as a restless multi-armed bandit (MAB) problem [30]. A MAB problem can be seen as a set of real distributions $B = \{R_1, ..., R_K\}$, with each distribution $R_k(1 \leq k \leq K)$ being associated with the rewards delivered by the k-th arm (i.e., decision options) and having a mean value of μ_k. A gambler iteratively plays one arm at a time and collects the associated reward. The objective is to maximize the sum of the collected rewards. For a given play strategy, the realized regret ρ after T plays is defined as follows:

$$R_{real}(T) = T\mu^* - \sum_{t=1}^{T}(\mu_{\alpha_t} - \beta_t c_{\alpha_t})$$

where $\mu^* = \max_{k=1}^{K} \mu_k$, α_t denotes the arm selected at time t, c_{α_t} is the cost of observing the reward of arm α_t, β_t is equal to 1 if the gambler observes the reward of α_t at time t and 0 otherwise.

In the mode selection problem, we can treat the rewards of the D2D mode and cellular mode as $-|\mathbb{E}_{D2D}|$ and $-|\mathbb{E}_{Up}| - |\mathbb{E}_{Down}|$ respectively, and then we can apply the History-Dependent Sequencing of Exploration and Exploitation (HD-SEE) [30] algorithm in mode selection. In particular, let $S_{k,t}$ be the number of reward observations for arm k by time t and $N_{k,t}$ be the number of times arm k has been selected by time t. The realized regret can be rewritten as follows:

$$R_{real}(T) = \sum_{k=1}^{K}(\triangle_k N_{k,T} + c_k S_{k,T})$$

where $\triangle_k = \mu^* - \mu_k$ is called the suboptimality gap of arm k. At each time t, the algorithm starts by calculating the estimated optimal arm:

$$\hat{k}_t^* = \arg\max_{k \in \mathcal{K}} \hat{\mu}_{k,t},$$

where $\hat{\mu}_{k,t}$ is the estimated mean reward of arm k by time t. Denoting the set of available arms as $\mathcal{K}$, then, for each arm $k \in \mathcal{K} - k_t^*$, it calculates the estimated suboptimality gap

$$\hat{\triangle}_{k,t} = \hat{\mu}_{k_t^*,t} - \hat{\mu}_{k,t}.$$

For each arm $k \in \mathcal{K}$, a control number $D_{k,t}$ is calculated based on the estimated suboptimality gap and the number of times that arm has been explored. For $k \in \mathcal{K} - k_t^*$ the control number is given as

$$D_{k,t} = \frac{L_2 \log(tK/\delta)}{J_{k,t}^2}$$

where

$$J_{k,t} = max\left\{0, \hat{\triangle}_{k,t} - 2\sqrt{\frac{L_1 \log(tK/\delta)}{\min(S_{k,t}, S_{k_t^*,t})}}\right\}.$$

Here $L_1 > 0$ and $L_2 > 0$ are constants. The control number for the estimated optimal arm k_t^* is calculated as

$$D_{k_t^*,t} = \frac{L_2 \log(tK/\delta)}{\min_{k \in \mathcal{K}-k_t^*} J_{k,t}^2}$$

For the selection process, if $S_{k,t} \geqslant D_{k,t}$ for all $k \in \mathcal{K}$, the algorithm chooses the arm $\hat{k}_t^*$, if not, the algorithm randomly chooses an arm for which $S_{k,t} < D_{k,t}$. In the mode selection problem, each BS only has two arms. Therefore, if $S_{k,t} \geqslant D_{k,t}$ holds for the suboptimal arm, the BS chooses the optimal arm; otherwise, the BS chooses the suboptimal arm.

In the HD-SEE algorithm, the number of times a suboptimal arm is chosen depends on the suboptimality gap of the arm. An arm with a larger suboptimality gap will be explored (i.e., chosen) fewer number of times compared to an arm with a smaller suboptimality gap. The regret in the HD-SEE algorithm is logarithmic in time, which is the best possible [30].

D. BS and UE Functional Orchestration

The main difference between cellular networks and ad hoc networks is the availability of BSes in cellular networks. Cellular networks also provide high-speed, out-of-band interconnections between BSes to exchange control signaling information (e.g., those needed for transmission scheduling). The availability of BSes and the high-speed, out-of-band interconnections in between provides the opportunity of having each BS collect information about network state information in its cell (e.g., local signal maps containing wireless channel gains and communication reliability across different links) through existing LTE BS-UE control signaling mechanisms, having BSes coordinate with one another in deciding network-wide transmission schedules, and then having each BS inform UEs in its cell of their transmission modes and schedules. This approach of placing core intelligence (i.e., decision making logic) at BSes and keeping UEs's functionality to the minimum of estimating communication reliability and maintaining local signal maps helps facilitate incremental deployment and technology evolution; this is because the number of BSes tend to be much less than that of UEs.

UCS also utilizes the inter-cell interference coordination (ICIC) mechanism of cellular networks to reduce control signaling overhead. The ICIC mechanism transmits some indicator message using the X2 interface to help with the scheduling process of neighboring BSes. The transmission along the X2 interface usually adopts high-speed wired networks such as optical fiber networks and does not consume wireless spectrum. Therefore, X2 interface transmission can be used to further reduce control signaling overhead in wireless channels. From the PRK interference model, to calculate the exclusion region for each link, the BS needs to know the receiver's local signal map and the value of Ks of the close-by links. However, some close-by links are in the neighboring cells and thus require inter-cell coordination. In UCS, the values of the PRK model parameter K and local signal maps are treated as the data part of the ICIC-related messages, and they are transmitted to the neighboring cell using the X2 interface to avoid using wireless resources. By the ICIC mechanism, transmission of inter-cell coordination control information no longer requires wireless transmissions.

E. Multi-Channel ONAMA Scheduling

Based on the interference relations between the uplinks, downlinks, and D2D links (if any as a result of mode selection) as identified by the PRK interference model, data transmissions along all the links can be scheduled in a unified manner to fully utilize the available wireless communication carriers. In particular, the objective of the unified scheduler is to schedule data transmissions so that a maximal set of non-interfering links are scheduled to transmit at each carrier and each time slot and that a link is scheduled to transmit only if there exists at least one data packet queued for transmission at the beginning of a time slot. Unlike existing cellular network scheduling algorithms which are based on a limited set of preconfigured frequency-division-duplexing (FDD) or time-division-duplexing (TDD) transmission patterns, the unified scheduler is adaptive to application traffic demand, and it ensures predictable communication reliability by respecting the interference relations as identified by the PRK model.

More specifically, the unified scheduler is based on the ONAMA TDMA scheduling algorithm [31]. ONAMA schedules a maximal set of non-interfering links to transmit at each time slot, but it is designed for single-carrier wireless networks, and it is not adaptive to traffic demand. In this study, we extend the ONAMA algorithm to consider the specific cellular network properties such as the availability of multiple carriers and base stations (BSes) as well as the traffic demand across individual links. Based on the BS and UE functional orchestration mechanism presented in Section III-D, each BS I knows the set of transmitters in its cell and the associated links L_I (whose receivers may be in a neighboring cell), and, for each such link i, the BS also knows the set of links M_i that interfere with link i. For each time slot t, the BS can also get the traffic demand d_i (i.e., number of data packets queued for transmission) for each link $i \in L_I$, and the BS knows the set of available carriers/channels RB. Then, the multi-channel transmission schedule for each time slot is identified by the BSes in a distributed manner as follows:

1) Each BS I initializes the state of each link $i \in L_I$ as UNDECIDED for each channel $rb \in RB$, and I also sets the state of every link in M_i as UNDECIDED for each channel;

2) Each BS I allocates the initial set of carriers to each link $i \in L_I$: if d_i is less than the average number of available channels (i.e., the total number of channels divided by the total number of links with non-zero transmission demand), denoted by $mean$, BS I allocates d_i channels to link i; if $d_i \geq mean$, BS I allocates $mean$ number of channels to link i. By this, the scheduler ensures the each link gets a fair share of the available transmission capacity.

3) For the pre-allocated channels, the BS assigns the maximum priority to the corresponding link i and sets its status as ACTIVE in those channels. If one link's demand has been satisfied, the BS sets it as INACTIVE in other channels.

4) For a link i whose demand has not been satisfied, the BS I computes a priority for each link $k \in M_i \cup i$ and each channel $rb \in RB$ for $d_k - mean$ times, which guarantees

the link with more remaining demand will be more likely to get the highest priority:

$$Prio.k.rb.d = Hash(k \oplus d \oplus t \oplus rb) \oplus k \oplus d, 1 \le d \le d_k,$$

where $Hash(x)$ is a message digest generator that returns a random integer by hashing x. Note the fourth and fifth XOR operator $\oplus$ are necessary for guaranteeing that all links' priorities are distinct even when $Hash()$ returns the same number on different inputs. This also means that a link with demand d_k will have $d_k - mean$ different priorities.

5) For each link $i \in L_I$, the BS I computes a priority for each link $k \in M_i \cup i$ and each channel $rb \in RB$:

$$Prio.k.rb = Max_{d=1}^{d_k - mean} Prio.k.rb.d$$

That is, each link $k \in M_i \cup i$ maintains a specific priority for each available channel rb.

6) For each link $i \in L_I$, the BS I iterates the following steps until the state of i in each channel is either ACTIVE or INACTIVE: A) for the channels in which the state of i is UNDECIDED, I tries to assign a different state to i in the increasing order of the IDs of the channels; for a given channel rb, if i's priority is higher than that of every other INACTIVE and UNDECIDED member in M_i, i's state is set as ACTIVE in channel rb, and its traffic demand d_i is reduced by one; conversely, if any ACTIVE member of $M_i \cup i$ has a higher priority than i, the state of i in channel rb is set as INACTIVE; if the traffic demand of i becomes zero, i's state is set as INACTIVE for each channel in which its state is UNDECIDED; B) the BS I shared the state of i with other BSes whose cells may have links that interfere with i.

7) If the state of a link i is ACTIVE for channel rb at time slot t, link i can transmit a data packet at channel rb and time slot t.

The details of the above multi-channel ONAMA scheduling algorithm for time slot t are shown in Algorithm 1.

Similar to the original ONAMA algorithm [31], the above algorithm can be readily shown to converge for each time slot. In particular, we have the following:

Theorem 1. *The set of all ACTIVE links at each time slot is a maximal set of non-interfering links for each channel.*

Proof. When the iteration terminates, a link is either ACTIVE or INACTIVE in each channel. For each INACTIVE link i in channel, there always exists an ACTIVE neighboring link in the set, whose priority is higher than that of i. Adding any additional link to the set of ACTIVE links for a given time slot - carrier resource block would end up with having two interfering links scheduled to transmit in the same time slot - carrier resource block , which is not allowed. Hence, The set of all ACTIVE links at a time slot t is a maximal set of non-interfering links in each channel.

$\square$

It usually takes a few rounds of coordination between close-by BSes for Algorithm 1 to converge to a transmission schedule for each time slot. Given that the number of BSes is

---

Algorithm 1 Multi-Channel ONAMA Scheduling at BS I

M_i: set of interfering links of a link $i \in L_I$;
d_k: traffic demand of link $k \in M_i \cup i$;
$mean$: average number of carriers available to links;
Perform the following actions for $\forall i \in L_I$:

1: state.i.rb = UNDECIDED, $\quad \forall rb \in RB$;
  Step 1: Preallocation
2: k.rb = $min\{d_k, mean\}, \forall k \in M_i \cup i$;
3: Prio.k.rb = $MAXIMUM, \forall rb \in k$;
4: state.k.rb = $ACTIVE, \forall rb \in k$;
5: **if** $d_k <= mean$ **then**
6:   state.k.rb = $INACTIVE, \forall rb \notin k$;
7: **end if**
  Step 2: Priority Calculation
8: Prio.k.rb.d = Hash(k$\oplus$ d$\oplus$ t$\oplus$ rb)$\oplus$ k$\oplus$ d,
9: $\forall k \in M_i \cup i, \forall rb \in RB, \forall d \in [1, d_k - mean]$;
10: Prio.k.rb = $Max_{d=1}^{d_k - mean}$ Prio.k.rb.d,
11: $\forall k \in M_i \cup i, \quad \forall rb \in RB$;
  Step 3: State Selection (i.e., Scheduling)
12: done = false;
13: **while** done == false **do**
14:   done = true;
15:   **for** each $rb \in RB$ in increasing order of rb ID **do**
16:     **if** $d_i - mean > 0$ && state.i.rb == UNDECIDED
17:       && Prio.i.rb > Prio.k.rb for each ACTIVE/
18:       UNDECIDED $k \in M_i$ **then**
19:       state.i.rb = ACTIVE;
20:       $d_i = d_i - mean - 1$
21:       **if** $d_i == 0$ **then**
22:         state.i.rb2 = INACTIVE, for each $rb2 \in$
23:         RB where state.i.rb2 == UNDECIDED;
24:       **end if**
25:     **end if**
26:     **if** Prio.i.rb < Prio.k.rb for any
27:       ACTIVE $k \in M_i$ **then**
28:       state.i.rb = INACTIVE;
29:     **end if**
30:     **if** state.i.rb == UNDECIDED **then**
31:       done = false;
32:     **end if**
33:   **end for**
34:   Share state.i.rb, $\forall rb \in RB$;
35:   Update state.k.rb, $\forall k \in M_i, \forall rb \in RB$ based on
36:    information from other BSes;
37: **end while**

---

usually much less than that of UEs, the convergence is much faster than if we have every UE participate in the scheduling process. Compared with the original ONAMA algorithm in [31], the multi-channel ONAMA scheduling algorithm does not need the exchange of state information between UEs and reduces the time for the decision. In addition, the preallocation not only ensures the fairness between different UEs, but also predetermines the state of the UE on certain RBs, reducing the number of iterations. These advantages make the multi-channel ONAMA scheduling run on the fly without the need for pre-computation.

Due to randomization in the above algorithm (e.g., in computing priorities), a link may well use different carriers across different time slots, and this channel hopping behavior can help improve resilience against channel fading and external interference. Additionally, the above algorithm considers traffic demands of different links, and a link with higher demands is more likely to get the highest priority to transmit.

IV. IMPLEMENTATION

The UCS framework is readily implementable in the 3GPP cellular architecture with minimal change to the existing LTE/5G standards. In what follows, we present our UCS implementation strategy in the open-source, standard-compliant cellular platform OpenAirInterface [32].

A. OpenAirInterface Platform

OpenAirInterface is an open-source prototyping and experimentation platform for LTE/5G cellular networks, and it can be used for systems simulation, systems emulation, and real-world deployment and measurement [32]. The default implementation of OpenAirInterface is compliant with the 3GPP standard (e.g., that for LTE), and the protocol stack of OpenAirInterface is shown in Figure 3. We implement the UCS framework by modifying the MAC component of OpenAirInterface.

Fig. 3. The OpenAirInterface protocol stack

B. Standard-Compliant Implementation of MAC Scheduler

In the 3GPP standards of LTE, the minimum scheduling unit is a Resource Block (RB) or RB Group depending on the bandwidth of the carrier. For example, if the bandwidth of the carrier is 1.4MHz, the minimum scheduling unit is one RB; if the bandwidth of the carrier is 5MHz, the minimum scheduling unit is two RBs that are called one RB group. There are two schedulers in the MAC layer, that is, the downlink scheduler and uplink scheduler. The two schedulers allocate , every 1ms (i.e., every LTE subframe), the minimum scheduling unit to each active UE according to the corresponding Channel Quality Indicator (CQI) and throughput demand.

The multi-channel PRK modeling, mode selection, and multi-channel ONAMA scheduling components of the UCS framework (see Figure 2) can be implemented in the MAC scheduler without any change to the existing LTE standard. In particular, we can implement the UCS framework by re-using the existing minimum scheduling unit definition and scheduler architecture. In the implementation, the UCS framework maintains two schedulers corresponding to uplink and downlink scheduling respectively to reduce the control

information overhead and to minimize the changes to the control information format. The downlink scheduler and uplink scheduler will update the interference relations between active links according to the updated K values and local signal maps. After that, the two schedulers know the links (both cellular links and D2D links) that can transmit concurrently in their scheduling period and then allocate a certain number of minimum scheduling units to them. The number of minimum scheduling units allocated depends on the data transmission demand and the multi-channel ONAMA scheduling algorithm.

The interference relations between D2D links and cellular links can be derived from their exclusion regions before scheduling. Therefore, UCS can guarantee predictable communication reliability along D2D links whether or not they transmit concurrently with downlinks or uplinks.

The execution of the MAC scheduler at a BS A requires A to know the local signal map of every node in its cell, the PRK model parameter K of every link in its cell, the local signal map of any node (i.e., BS or UE) in a neighbouring cell whose transmission may interfere with any link of A's cell, and the PRK model parameter K of any link in a neighbouring cell that may be interfered by a transmission in A's cell. This is achieved through BS-UE coordination and inter-BS coordination as we discuss next.

C. Control Channel

The BS-UE coordination achieved mainly by the physical downlink control channel (PDCCH) and physical uplink control channel (PUCCH). The PDCCH is used to signal downlink scheduling assignments and uplink scheduling grants. The maximum size of the control region for the downlink is normally three OFDM symbols (four in the case of narrow cell bandwidths) in each subframe. Similar to the LTE downlink, there is also a need for uplink control signaling to support downlink and uplink transport channels. The information in the PUCCH is the combination of the hybrid-ARQ acknowledgements, channel-state reports, and scheduling requests. Unlike downlink control signaling, uplink control signaling is transmitted along the uplink whether or not the UE has any uplink transport-channel data to transmit.

To support the BS-UE coordination in the UCS framework, we need to change the control information format in the PDCCH and PUCCH. In the PDCCH, we define the local signal feedback flag (1 bit) and local terminal indicator (16 bits). The BS requests an aperiodic local signal map update by setting the local signal feedback as 1 and transmit the active local terminal's identity in the local terminal indicator. In the PUCCH, we define the local signal map indicator (4 bits for each terminal). When the UE receives the local signal map update request from the PDCCH, it will modify the channel gain from the local active terminals to 4 bits and report them in the local terminal indicator following the sequence of terminals in the local terminal indicator.

D. Extension of X2 Interface for ICIC

LTE standards are defined such that factor-one frequency reuse is possible. To help mitigate inter-cell interference, the

X2 interface is defined for Inter Cell Interference Coordination (ICIC) and enhanced ICIC (eICIC), and control signaling messages have been defined for the X2 interface. For instance, control messages with High Interference Indicator (HII) and Overload Indicator (OI) have been defined for coordinating uplink transmissions, and control messages with Relative Narrowband Transmit Power (RNTP) have been defined for coordinating downlink transmissions.

The existing X2 signaling messages are unable to indicate precise interference relations between links involving UEs of different cells, thus unable to support predictable interference control and communication reliability as required by mission-critical applications. To enable predictable interference control in cellular networks, we extend the X2 interface by defining a new X2 message *PRK-Signal* to support the implementation of the UCS framework. When a PRK-signal message is sent from one BS to its neighbouring BSes, the message includes the local signal map of every node (including UEs and the BS) in the sending BS cell as well as the PRK model parameter K of every link in the sending BS cell. Based on the information contained in the PRK-signal messages exchanged between BSes, BSes can derive the interference relations between links and then schedule transmissions according to the multi-channel ONAMA algorithm presented earlier. To support the implementation of the multi-channel ONAMA algorithm, we also define an X2 message *TX-Status* by which a BS shares the status (i.e., UNDECIDED, ACTIVE, or INACTIVE) of every link in its cell.

V. MEASUREMENT EVALUATION

We have implemented the UCS framework in the OpenAir-Interface cellular network platform [32]. In this section, we evaluate the feasibility and effectiveness of UCS using the software-defined radios (SDRs) of the ORBIT wireless testbed, to validate that the UCS framework and its implementation actually work with real-world platforms. In Section VI, we will evaluate UCS in a comprehensive manner through at-scale, high-fidelity simulation studies.

A. SDR Deployment of UCS in ORBIT

To validate the feasibility and effectiveness of realizing the UCS framework with the LTE-compatible OpenAirInterface platform and commodity hardware, we deploy our OpenAirInterface implementation with the USRP B210 software-defined-radio (SDR) hardware platform of the ORBIT wireless testbed.

ORBIT is designed for realistic evaluation of protocols and applications, and it has a 20×20 two-dimensional grid of programmable radio nodes which can be interconnected into different topologies. Orbit has eight USRP B210 SDR nodes that can be used to form a cellular network, and the locations of the eight nodes are shown in Figure 4.

We evaluate the UCS framework using the ORBIT B210 SDRs in a single-cell scenario and a multi-cell scenario respectively. In the single-cell scenario, we set node 3 as the BS and the remaining nodes as the UEs. To create links of different types and for comprehensive evaluation of different components of the UCS framework, we create a downlink from

node 3 to node 4, two uplinks from node 2 and node 6 to node 3 respectively, and two UE-to-UE communication pairs from node 5 to node 7 and from node 1 to node 8 respectively. In the multi-cell scenario, we set node 1 and node 8 as the BSes, and we create a downlink from node 1 to node 7 and an uplink from node 2 to node 8. In addition, we create two UE-to-UE communication pairs from node 5 to node 3 and node 4 to node 6 respectively. We set the transmission power as 95dBm and system bandwidth as 10MHz (25RBs). We set the minimum communication reliability requirement as 90% in the study.
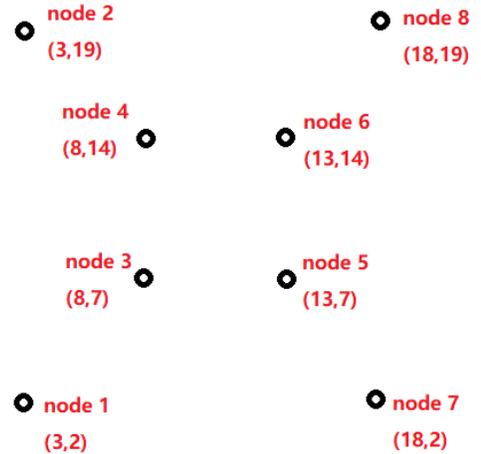
Fig. 4. the location of nodes on the ORBIT platform

B. Measurement Results

For clarity of presentation, we use $\langle A, B \rangle$ to denote a unidirectional link/transmission from node A to B in Figures 5 - 10.

For the two UE-to-UE communication pairs of the single-cell scenario, the BS determines their communication mode according to the logic specified in Section III-C and based on exclusion region size of different communication modes. In our study, node 5 transmits packets to node 7 directly (i.e., in D2D mode), while node 1 transmits packets to node 8 via the BS (i.e., in cellular mode). Figure 5 shows exclusion region sizes of different communication modes for the two UE-to-UE communication pairs. We see that the exclusion region size of the cellular mode is greater than that of the D2D mode for the link from node 5 to node 7, thus they transmit to each other directly to improve the network throughput. For the link from node 1 to node 8, it has the same exclusion region size for the D2D mode and cellular mode in our study. To reduce transmission power consumption and to add to the diversity of communication modes present in the experiment, we set the transmission mode as cellular mode so that the transmission goes through the BS (i.e., node 3).

Figure 6 shows the actual communication reliability along each communication link/pair in the single-cell scenario. We see that UCS ensures the required communication reliability
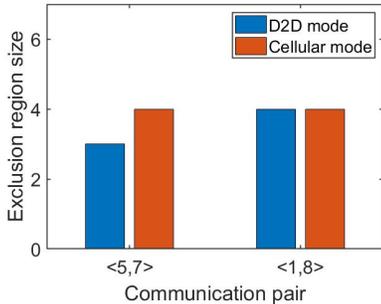
Fig. 5. Exclusion region size of UE-to-UE communication pairs in single-cell scenario
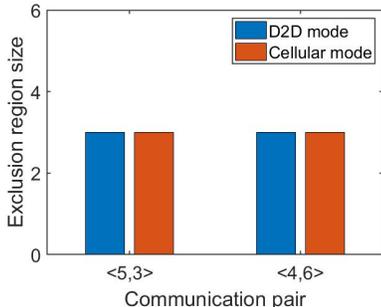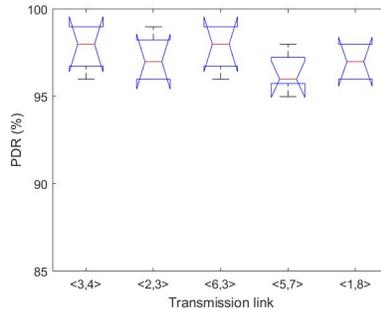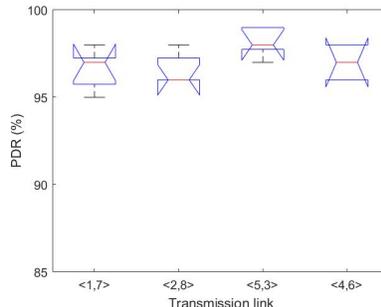

Fig. 6. Communication reliability in single-cell scenario

Fig. 7. Communication reliability comparison: importance of proper scheduling via UCS
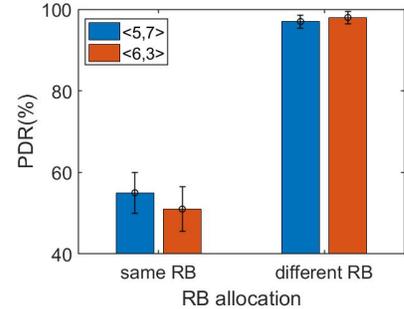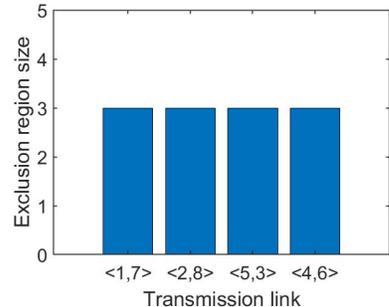

Fig. 8. Exclusion region size of UE-to-UE communication pairs in multi-cell scenario

Fig. 9. Communication reliability in multi-cell scenario

Fig. 10. Exclusion region size for each link in multi-cell scenario

for all the communication links/pairs. In the network setup, the D2D link $\langle 5, 7 \rangle$ and the cellular link $\langle 6, 3 \rangle$ interfere with each other. To show the importance of proper scheduling via UCS, we run an experiment where links $\langle 5, 7 \rangle$ and $\langle 6, 3 \rangle$ use the same RB, and compare result with that of using UCS in which the two links use different RBs. Figure 7 shows the corresponding communication reliability and along the two links. We see that, by using different RBs for the two mutually-interfering links, UCS ensures a reliability no less than the minimum required reliability of 90%, while the method of using the same RB for the two links leads to very low communication reliability which does not meet the application requirement.

In the multi-cell scenario, Figure 8 shows the exclusion region sizes of the different communication modes for the two UE-to-UE communication pairs. The D2D and cellular modes have the same exclusion region sizes for both communication pairs. In our study, we set the communication modes of both links as D2D so that the experiment setup has at least one D2D link in each cell, as expected in real-world settings.

Figures 9 and 10 show the communication reliability along each link and the exclusion region size of each link in the multi-cell scenario respectively. We see that, similar to the single-cell scenario, UCS ensures the application-required minimum communication reliability of 90%. In particular, the inter-cell coordination mechanism of UCS (see Section IV-D) ensures that mutually-interfering links of different cells do not use the same RB in transmission too.

VI. SIMULATION EVALUATION

Having validated the feasibility and effectiveness of realizing the UCS framework using commodity software and hardware platforms, here we use the simulator of OpenAirInterface to evaluate the performance of UCS with at-scale, high-fidelity simulation.

A. Methodology

Simulation platform OpenAirInterface comes with a high-fidelity simulator for OpenAirLTE networks. The OpenAirInterface simulator enables simulation with the full PHY layer and synthetic radio channels, or with a PHY layer abstraction. In both PHY layer simulation modes, the full protocol stack of the UCS-variant of LTE is executed as is the case with USRP B210 hardware implementation and validation. The PHY layer of the OpenAirInterface provides the abstraction for all the transmission channels in LTE and the simulation for a large amount of channel types (e.g., Rayleigh, Rice and AWGN) with different parameter settings, which can cover a variety of actual scenarios. Consequently, the simulation in OpenAirInterface has a high degree of fidelity.

Simulation Scenarios We focus on multi-cell scenarios where a total of 135 UEs are distributed in 9 cells, which are organized in a 3×3 grid manner such that each cell covers a square area of $500m \times 500m$ and the 9 cells covers a square area of $1,500m \times 1,500m$. Each cell has 15 UEs deployed; five UEs are randomly chosen to communicate with the BS directly, forming five cellular links, with both uplink and downlink data transmissions; the remaining 10 UEs

form five UE-to-UE communication pairs, with the source UE and destination UE randomly picked. Each UE-to-UE communication pair can be in cellular mode or D2D mode, with the specific mode to be selected by UCS.

To understand the behavior of UCS in different network settings, we experiment with both random and grid network topologies, where the UEs of each cell are spatially distributed in a uniform-random and grid manner respectively. The base station (BS) of each cell is located at the center of the cell. We also experiment with different LTE channel models of different path-loss exponents and fading models. To study UCS' capability of ensuring predictable control of interference and thus predictable communication reliability, we experiment with different packet-delivery-reliability (PDR) requirements of 80%, 85%, 90%, and 95%. To stress-test the interference control behavior of UCS, we consider the saturated traffic model where a node always has a packet to transmit.

Table II summarizes the key parameters used in the aforementioned simulation configurations. Note that the simulation configurations are meant to create multi-cell settings mimicking real-world scenarios. To understand the behavior of UCS in heterogeneous network settings, we also study the scenario where each UE randomly chooses a PDR requirement of 80%, 85%, 90%, or 95%, as well as the scenario where each transmitter randomly chooses a transmission power of 15dBm, 20dBm, or 25dBm.

TABLE II
PARAMETERS USED IN OPENAIRINTERFACE SIMULATION

Parameter	Value
# of eNBs (i.e., base stations)	9
# of UEs	135
Area of each cell	$500m \times 500m$
Topology	random, grid
# of carriers sharing a K	25, 50, 100
Path-loss exponent	3.0, 3.5, 4.0
Fading type	Rayleigh, Rice, AWGN
eNB transmission power	40dBm
UE transmission power	20dBm
Frequency band	band 7 (center freq.: 2.6GHz)
Simulation duration	10000 TTIs
# of runs per expt. config.	10

Scheduling Protocols To understand the effectiveness of the UCS scheduling framework in ensuring predictable communication reliability and high channel spatial reuse, we compare it with the following scheduling protocols:

- *I*AS: an interference-aware scheduling scheme that exploits the multi-user diversity of the cellular network such that the performance of the D2D underlay is optimized while maintaining a target performance level of the cellular network. The D2D terminals sense the radio spectrum and aid the BS in generating local awareness of the radio environment. The BS then uses this information in interference-aware resource allocation among the cellular and D2D links [7].
- *Q*AS: a QoS-aware scheduling scheme that utilizes channel statistical characteristics to maximize the overall throughput of the cellular users and admissible D2D pairs while guaranteeing a target signal-to-interference-plus-noise ratio (SINR) for each receiver. A D2D receiver only

feeds back the channel-state-information (CSI) for a few best potential partner cellular users to reduce feedback overhead [8].

For understanding the optimality of the UCS scheduling framework, we also compare it with *iOrder* [27], a state-of-the-art centralized scheduling scheme that maximizes channel spatial reuse while ensuring the required PDRs by considering both the interference budget (i.e., tolerable interference power at receivers) and queue length in scheduling. When constructing the schedule for a time slot, iOrder first picks a link with the maximum number of queued packets; then iOrder adds links to the slot one at a time in a way that maximizes the interference budget at each step; this process repeats until no additional link can be added to the slot in any communication channel without violating the application requirement on link reliability [27]. When experimenting with iOrder, we assume that all the channel state information is available (which is unrealistic but serves as a reference for understanding the optimality of UCS), and we use the same set of cellular links and D2D links as those in the experiments for UCS. (Note: the original iOrder algorithm was designed for single-channel settings. We extend it to multi-channel settings in this study by using the core idea of the iOrder algorithm in centrally scheduling concurrent transmissions for each channel.)

Simulation results To understand UCS' capability in ensuring predictable communication reliability, we measure the actual packet-delivery-reliability (PDR) when using a same PRK model parameter K for different number of carriers (i.e., 25, 50 and 100). From Figures 11 and 12, we see that maintaining one K for 25 and 50 adjacent carriers can ensure application required PDRs. Figure 13 shows that maintaining one K for 100 adjacent carriers also can also guarantee PDRs up to 90%, but it does not always ensure the required high PDR of 95%. We see that, by choosing the right number n of carriers/channels for which to maintain a single PRK model parameter K, UCS can ensure the required PDRs. The fact that too large a n (i.e., 100 in this study) cannot always ensure the required high PDRs also demonstrate the tradeoff between control signaling overhead, modeling accuracy, and protocol performance, as discussed in Section III-B. For the figures in the rest of this section, we use the data for scenarios when UCS maintains a PRK model parameter K for every 25 adjacent carriers.

The reason why UCS ensures the required communication reliability is because it adapts the PRK model parameter and the thus the size of the exclusion region (ER) around each receiver (i.e., number of nodes in the ER) according to the application-required PDR and in-situ network and environmental conditions. As shown by Figures 14 and 15 for cellular links and D2D links respectively, higher PDRs are achieved by increasing the value of parameter K and thus expanding the ER size.

To understand the frequency reuse efficiency for the mode selection algorithm of the UCS framework, Figure 16 shows, for the set of UE-to-UE communication pairs operating in the D2D mode, the ER size in the cellular mode minus that in the D2D mode, with the ER size for the cellular mode
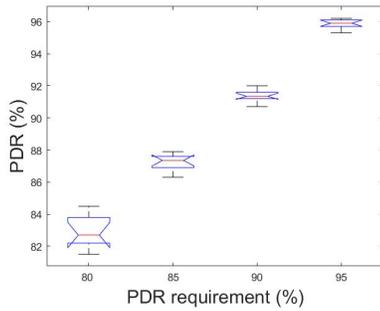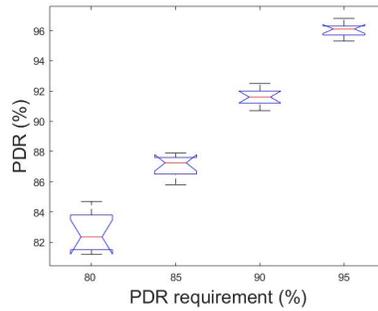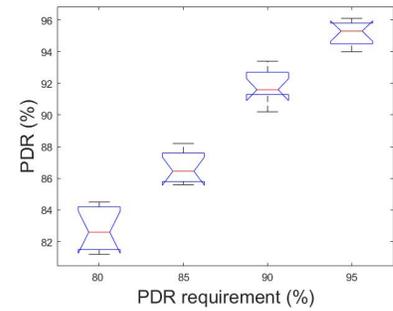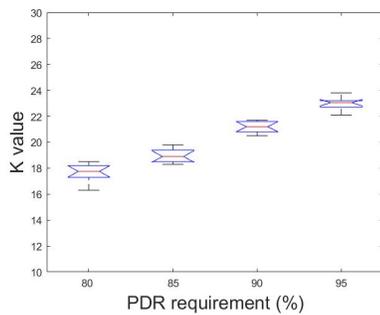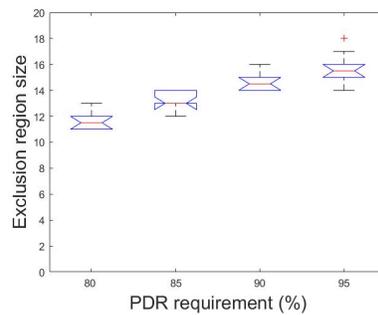
Fig. 11. Same K for adjacent 25 carriers

Fig. 12. Same K for adjacent 50 carriers

Fig. 13. Same K for adjacent 100 carriers

Fig. 14. Value of parameter K
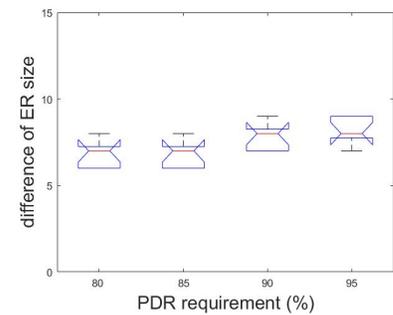

Fig. 15. Exclusion region size

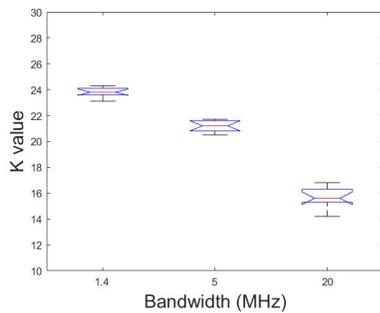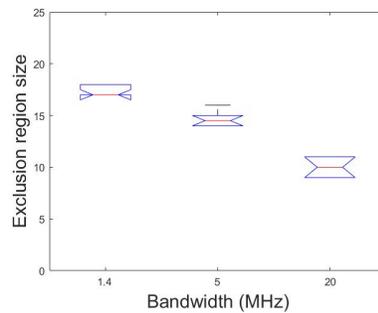Fig. 16. Comparison of ER size in D2D and cellular modes for UE-to-UE pairs choosing D2D mode

Fig. 17. The value of the parameter K for different bandwidth

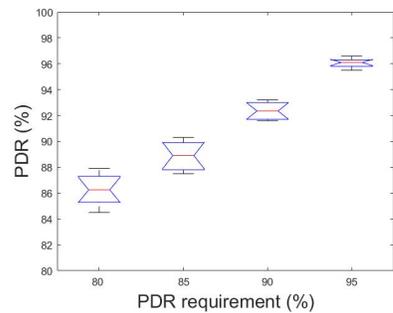Fig. 18. Exclusion region size for different bandwidth

Fig. 19. Communication reliability in heterogeneous reliability scenario
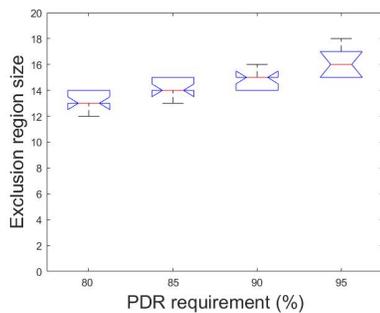
Fig. 20. Exclusion region size in heterogeneous reliability scenario
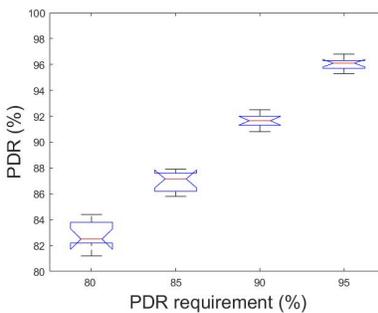
Fig. 21. Communication reliability in heterogeneous power scenario
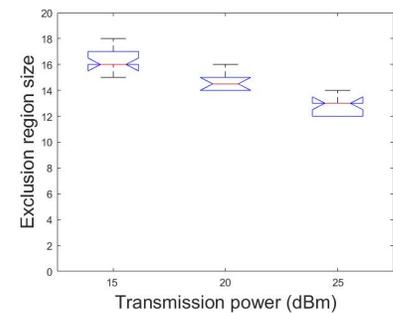
Fig. 22. Exclusion region size in heterogeneous power scenario
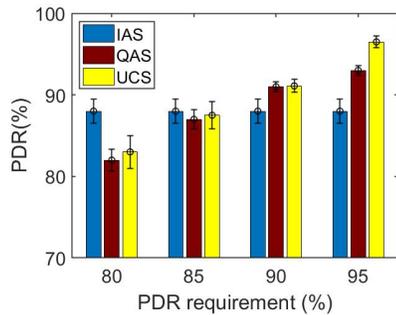
Fig. 23. Predictable reliability guarantee for random topology
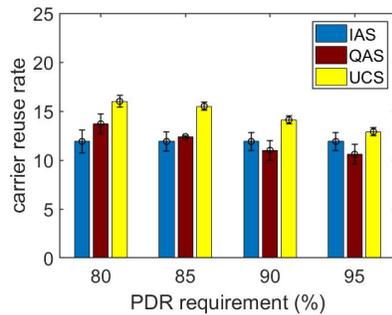
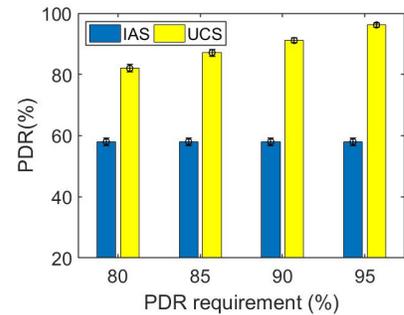Fig. 24. Mean carrier reuse rate with the random topology

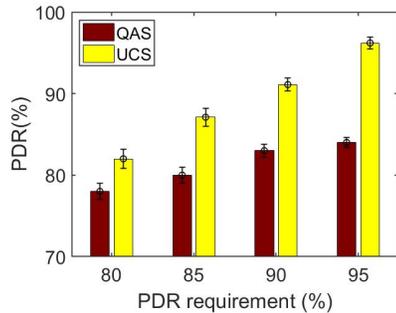Fig. 25. Predictable reliability guarantee comparison with IAS

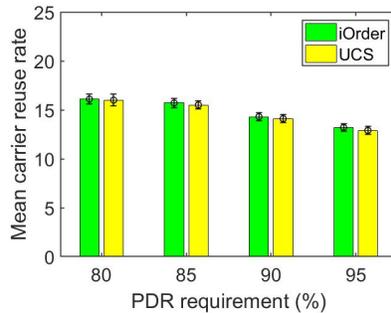Fig. 26. Predictable reliability guarantee comparison with QAS

Fig. 27. Comparison with iOrder under the random topology
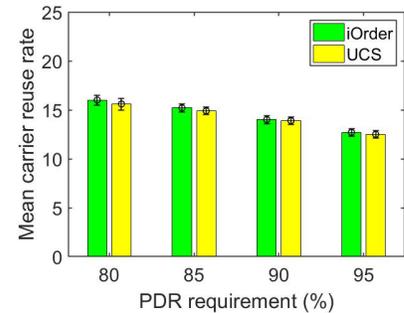

Fig. 28. Comparison with iOrder under the grid topology

calculated as the sum of the ER sizes of the involved uplink and downlink. We see that, for these communication pairs, operating in the D2D mode significantly reduces the ER size and thus improves the transmission concurrency and channel spatial reuse.

To understand the effect of the number of available carriers on the behavior of UCS, we compared the value of parameter K and the size of exclusion region when different communication bandwidth is used. For instance, Figure 17 and 18 shows the values of K and ER size when the communication PDR requirement is 90%. With the increase of available carriers, the interference between concurrent transmitting links decreases. Accordingly, UCS reduces the size of exclusion regions by adjusting the value of parameter K dynamically to ensure the required communication reliability while maximizing carrier spatial reuse.

For the heterogenous network setting where each link randomly chooses a PDR requirement, Figures 19 and 20 show the communication reliability and corresponding ER size for each reliability requirement. We see that UCS ensures application-required PDR in these settings too. Compared with the homogeneous scenario where each link has the same PDR requirement, the average communication PDR of some links with lower reliability requirements (e.g., 80%) is a little higher. This is because the heterogeneous setting has more links with higher reliability requirements, which tend to have larger ERs as reflected in Figure 20.

For the heterogenous network setting where each transmitter randomly picks a transmission power, Figure 21 shows the communication reliability in UCS. We see that UCS ensures application-required PDR. For the communication pairs with

PDR requirement of 90%, Figure 22 shows the ER size for links with different transmission powers. We see that transmission power can influence the ER size, and thus affecting communication concurrency and throughput. The links with the lower transmission power tend to tolerate lower interference power, thus they maintain larger ERs to guarantee the required communication reliability.

Figures 23 and 24 show the PDR and carrier reuse rate in different protocols respectively. We see that the existing cellular protocols IAS and QAS cannot ensure predictable interference control (as explained in Section I) and thus cannot ensure predictable communication reliability, for instance, not able to ensure the required high reliability of 95%.

To highlight the advantages of UCS in the predictable communication reliability guarantee, we further compared UCS with IAS and QAS separately in Figure 25 and Figure 26 in different network setting. In Figure 25, we reduced the area of each cell to $150m * 150m$ to increase the interference of concurrent transmission links; IAS cannot even guarantee the communication reliability up to 60% because it only avoids the strong interference, not considering the interference accumulation. In Figure 26, we changed the channel type from Rayleigh model to Rice model; QAS cannot guarantee the communication reliability up to 85% because it only targets for Rayleigh model, not considering potentially different channel models and reality. In contrast, UCS ensures the required PDR for different cell ranges and channel models while achieving a higher carrier reuse rate (which is defined as the number of links using a carrier at each time slot). In fact, Figures 27 and 28 show the distributed UCS scheduling framework achieves a carrier reuse rate statistically equal to

that of the centralized, state-of-the-art scheduling algorithm iOrder, showing the optimality of the UCS framework [1].

VII. Conclusion

We have proposed a field-deployable, unified cellular scheduling framework UCS to ensure predictable communication reliability in cellular networks with D2D links. The UCS framework effectively leverages the PRK interference model and addresses the challenges of multi-channel PRK-based scheduling in cellular networks. UCS provides a simple mode selection mechanism which, together with PRK-based cellular scheduling, maximizes communication throughput while ensuring communication reliability. UCS also effectively leverages cellular network structures (e.g., the availability of BSes and high-speed, out-of-band networks in-between) to orchestrate BS and UE functionalities for light-weight control signaling and ease of incremental deployment and technology evolution. The feasibility and performance of UCS have been verified through high-fidelity simulation and real-world hardware and software implementation.

References

[1] E. Dahlman, S. Parkvall, and J. Skold, *4G, LTE-Advanced Pro and The Road to 5G*. Academic Press, 2016.

[2] S. Essakiappan, S. Harb, and A. Solar-schultz, "Machine-Type Communications: Current Status and Future Perspectives Toward 5G Systems," *IEEE Communications Magazine*, September 2015.

[3] M. N. Tehrani, M. Uysal, and H. Yanikomeroglu, "Device-to-device communication in 5G cellular networks: challenges, solutions, and future directions," *IEEE Communications Magazine*, may 2014.

[4] H. Zhang, X. Liu, C. Li, Y. Chen, X. Che, L. Y. Wang, F. Lin, and G. Yin, "Scheduling with predictable link reliability for wireless networked control," *IEEE Transactions on Wireless Communications*, vol. 16, no. 9, 2017.

[5] H. Zhang, X. Che, X. Liu, and X. Ju, "Adaptive instantiation of the protocol interference model in wireless networked sensing and control," *ACM Transactions on Sensor Networks (TOSN)*, vol. 10, no. 2, 2014.

[6] J. R. Moyne and D. M. Tilbury, "Control and communication challenges in networked real-time systems," *Proceedings of the IEEE*, vol. 95, no. 1, 2007.

[7] P. Janis, V. Koivunen, C. Ribeiro, J. Korhonen, K. Doppler, and K. Hugl, "Interference-aware resource allocation for device-to-device radio underlaying cellular networks," in *Vehicular Technology Conference, 2009. VTC Spring 2009. IEEE 69th*. IEEE, 2009.

[8] D. Feng, L. Lu, Y.-W. Yi, G. Y. Li, G. Feng, and S. Li, "Qos-aware resource allocation for device-to-device communications with channel uncertainty," *IEEE Transactions on Vehicular Technology*, vol. 65, no. 8, 2016.

[9] H. Min, J. Lee, S. Park, and D. Hong, "Capacity enhancement using an interference limited area for Device-to-Device uplink underlaying cellular networks," *IEEE Transactions on Wireless Communications*, vol. 10, no. 12, 2011.

[10] Q. Ye, M. Al-Shalash, C. Caramanis, and J. G. Andrews, "Distributed resource allocation in Device-to-Device enhanced cellular networks," *IEEE Transactions on Communications*, vol. 63, no. 2, 2015.

[11] Q. Ye, M. Al-shalash, C. Caramanis, and J. A. and, "Distributed Resource Allocation in Device-to-Device Enhanced Cellular Networks," *IEEE Transactions on Communications*, vol. 63, no. 2, 2015.

[12] L. Lei, Y. Kuang, X. Shen, C. Lin, and Z. Zhong, "Resource control in network assisted Device-to-Device communications: Solutions and challenges," *IEEE Communications Magazine*, vol. 52, no. 6, 2014.

[13] W. Wang, F. Zhang, and V. K. N. Lau, "Dynamic power control for delay-aware Device-to-Device communications," *IEEE Journal on Selected Areas in Communications*, vol. 33, no. 1, 2015.

[14] Y. Cui, V. K. N. Lau, R. Wang, H. Huang, and S. Zhang, "A Survey on Delay-Aware Resource Control for Wireless Systems: Large Deviation Theory, Stochastic Lyapunov Drift, and Distributed Stochastic Learning," *IEEE Transactions on Information Theory*, vol. 58, no. 3, 2012.

[15] D. Verenzuela and G. Miao, "Scalable D2D Communications for Frequency Reuse >>1 in 5G," vol. 16, no. 6, 2017.

[16] S. Lv, C. Xing, Z. Zhang, and K. Long, "Guard Zone Based Interference Management for D2D-Aided Underlaying Cellular Networks," *IEEE Transactions on Vehicular Technology*, vol. 66, no. 6, 2017.

[17] K. Doppler, M. Rinne, C. Wijting, C. B. Ribeiro, and K. Hugl, "Device-to-device communication as an underlay to LTE-advanced networks," *IEEE Communications Magazine*, vol. 47, no. 12, 2009.

[18] T. Peng, Q. Lu, H. Wang, S. Xu, and W. Wang, "Interference avoidance mechanisms in the hybrid cellular and device-to-device systems," in *Personal, Indoor and Mobile Radio Communications, 2009 IEEE 20th International Symposium on*. IEEE, 2009.

[19] C.-H. Yu, K. Doppler, C. Ribeiro, and O. Tirkkonen, "Performance impact of fading interference to device-to-device communication underlaying cellular networks," in *Personal, Indoor and Mobile Radio Communications, 2009 IEEE 20th International Symposium on*. IEEE, 2009.

[20] D. López-Pérez, X. Chu, A. V. Vasilakos, and H. Claussen, "On distributed and coordinated resource allocation for interference mitigation in self-organizing lte networks," *IEEE/ACM Transactions on Networking*, vol. 21, no. 4, pp. 1145–1158, 2013.

[21] Y. Niu, C. Gao, Y. Li, L. Su, D. Jin, and A. V. Vasilakos, "Exploiting Device-to-Device Communications in Joint Scheduling of Access and Backhaul for mmWave Small Cells," *IEEE Journal on Selected Areas in Communications*, vol. 33, no. 10, pp. 2052–2069, 2015.

[22] M. Ding, D. Lopez-Perez, R. Xue, A. V. Vasilakos, and W. Chen, "On dynamic time division duplex transmissions for small cell networks," arXiv:2006.14829v1, 2020.

[23] E. Dahlman, S. Parkvall, and J. Skold, *4G LTE/LTE-Advanced for Mobile Broadband*. Elsevier Ltd, 2011.

[24] H. Min, W. Seo, J. Lee, S. Park, and D. Hong, "Reliability improvement using receive mode selection in the device-to-device uplink period underlaying cellular networks," *IEEE Transactions on Wireless Communications*, vol. 10, no. 2, 2011.

[25] R. Z. (Editor), *Industrial Communication Technology Handbook*. CRC Press, 2015.

[26] A. Saifullah, Y. Xu, C. Lu, and Y. Chen, "Real-time scheduling in WirelessHART networks," in *IEEE RTSS*, 2010.

[27] X. Che, H. Zhang, and X. Ju, "The case for addressing the ordering effect in interference-limited wireless scheduling," *IEEE Transactions on Wireless Communications*, vol. 13, no. 9, 2014.

[28] C. Li, H. Zhang, T. Zhang, J. Rao, L. Y. Wang, and G. Yin, "Cyber-physical scheduling for predictable reliability of inter-vehicle communications," *IEEE Transactions on Vehicular Technology*, vol. 69, no. 4, 2020.

[29] L. Wang, H. Zhang, and P. Ren, "Distributed scheduling and power control for predictable iot communication reliability," in *IEEE ICC*, 2018.

[30] C. Tekin, M. Liu *et al.*, "Online learning methods for networking," *Foundations and Trends® in Networking*, vol. 8, no. 4, 2015.

[31] X. Liu, Y. Chen, and H. Zhang, "A maximal concurrency and low latency distributed scheduling protocol for wireless sensor networks," *International Journal of Distributed Sensor Networks*, vol. 11, no. 8, 2015.

[32] N. Nikaein, M. K. Marina, S. Manickam, A. Dawson, R. Knopp, and C. Bonnet, "OpenAirInterface: A Flexible Platform for 5G Research," *ACM SIGCOMM Computer Communication Review*, vol. 44, no. 5, 2014.

---

[1]The carrier reuse rates in the random and grid networks are statistically similar.